We thank the reviewer for their comments. Below is our point by point response in blue.

We draw the reviewer's attention to the fact that, following a similar comment of all reviewers, a figure 1 has been added to the manuscript, featuring information on the operation statistics of DDU lidar. Therefore, all figure numbers have been incremented accordingly as compared to the first version of the manuscrit.
Also, to address another comment, the threshold temperatures T_{NAT}, T_{STS} and T_{ICE} are now computed based on the closest MLS H_2O and HNO_3 concentration measurement. Although this does not change their meaning or their interpretation, most of the figures have gone through some slight changes.

General / major comments:

G1) The lidar at Dumont d'Urville is in operation since 1989, why do you only focus on the last 14 year? Did the occurrence of PSCs in general and of different PSC types changed since 1989? Do you observe a trend since 1989?
Even if the original setup of the lidar dates back to 1989, it has not been in continuous operation since then. Still, it is continuously operating since 2006 with the same laser source installed in 2005. The monitoring calendar has also been greatly enhanced from 2007 onwards, providing a consistent time series motivating the choice of this time period, also coincident with the launch of the CALIPSO mission. As a whole, spaceborne coverage and recent version of the products are also actually better on this time frame. In the 1989-2006 time period, the monitoring policy was different partly due to the presence of a colocated ozone lidar. As mentionned in the paper line **513-514**, no significant PSC trend was established in the 1989-2008 time interval from David et al., (2010)". The manuscript has been edited accordingly, line **80**: "Considering the latest laser source replacement in 2005 and the continuous monitoring from 2006, ..."

G2) It would be good if the authors could add a paragraph about the lidar measurements including some statistics, e.g. How many days per year the lidar was operational? How many PSC were observed per year? When were there observed? Are the PSC observation evenly distributed over the winter?...
Following the comment of another reviewer we included statistics on the operation of DDU lidar. The newly aded figure 1 presents the number of measurement days per year, from 2007 to 2020 as well as the duration of these measurements per month, in average. The number of PSC days observed per year is represented by the red triangles of figure 9. The temporal distribution of PSC occurences during the winter season does not support the core of the analysis around the PSC type distribution using different classification schemes, and we choose not to include it in this study.
Here is the new Figure 1:

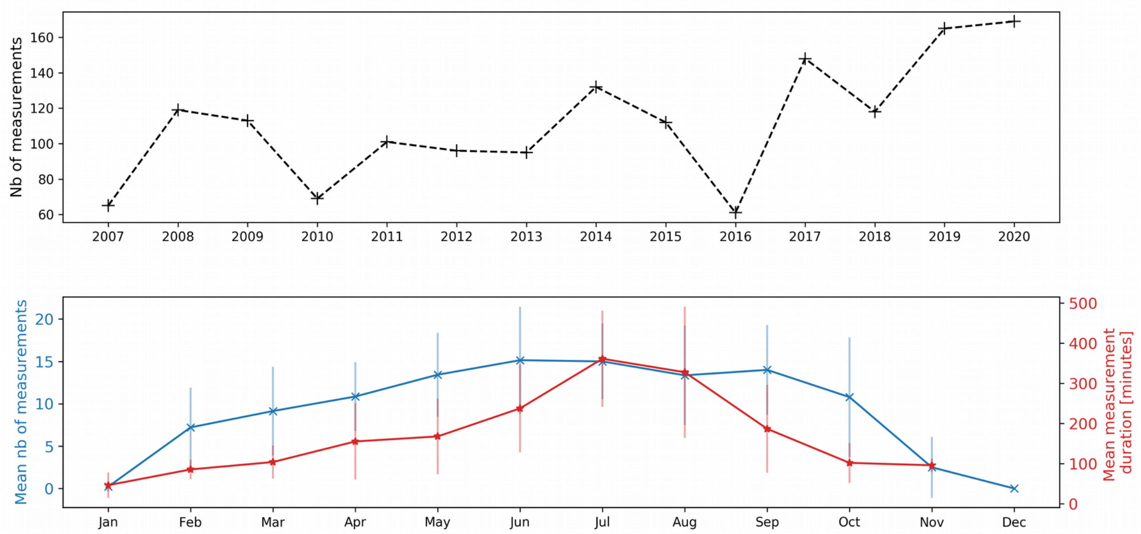

Figure 1: Operation statistics of DDU lidar. (a) Number of measurement days per year, from 2007 and to 2020 and (b) mean duration of measurement sessions per month, in minutes, from 2007 to 2020.

G3) Please include a more detail analysis of the 14-year dataset: e.g. year to year variability, comparison to other ground-based stations and CALIPSO
We address here and below the comments on year-to-year variability as a whole, and comparison to other groundbased and spaceborne datasets:
A statistical analysis on the interannual variability is provided to an extent in the trend analysis, which precisely includes features the statistics asked by the reviewer: year-to-year PSC variability at DDU. A interannual variability of the PSC type distribution would use smaller samples not robust enough to produce reliable statistics so we choose not include it.

Other reviewers mentioned the need to compare with other groundbased datasets. It is now included between lines **341** and **354** where the types distribution we observe at DDU is compared to those observed at McMurdo (2006-2010) and Concordia (2014-2018) by Snels et al., (2019 and 2021) respectively.

As mentioned in our response to the other reviewers, we did a mistake when reading Tesche et al. (2021) and did not realize that while all winters from 2006 to 2018 are considered for the Arctic stations, only 2012 and 2015 are used for Antarctica. To address this issue, we extracted the CALIOP PSC Mask v2 product around DDU and included it in the study. To do so, we used a method pretty similar to the one described by Snels et al. (2021) when comparing groundbased measurements from Concordia with CALIOP measurements.

In the reviewed PSC distribution, we count the PSC layers for each type. Introducing a comparison with CALIOP measurements led us to adapt our counting approach. Since CALIOP sorts each vertical bin separately (with a coherence criterium), it takes the geometrical thickness of PSC into account. This is relevant and we modified our method accordingly. Therefore, we now take into account each vertical bin of the identified PSC layer as explained in section 3.2. This explains the change in the distribution in figure 3 since this reviewed version.

To include this new content in the mansucript, a presentation of CALIOP was included at lines **140-147**. A presentation of the method of PSC detection with CALIOP is included at lines **202-223**. Finally, the types distribution produced for DDU for 2012 and 2015 was replaced in Figure 3d by the CALIOP data extraction and the subsequent discussion has been edited (lines **296-309**, **311-312** and **335-338**).

Even if we don't consider yearly PSC types distribution, the interannual variability of PSC occurences is displayed in Figure 9 as red triangles marks. Besides, the new version of Figure 9 now includes the number of CALIOP PSC days at DDU, merely above 10 per year.

Here is the new version of Figure 9:

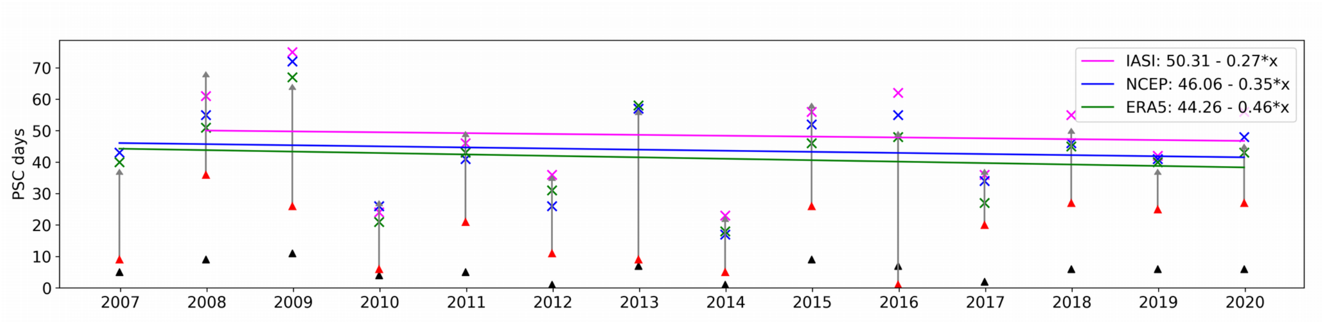

Figure 9: PSC days per year at DDU from 2007 to 2020 featuring PSC detection with the lidar in red triangles. Potential PSC days per year estimated by ERA5, NCEP and IASI based on the lidar measurements are shown in green and red respectively. Green, blue and fuchsia lines represent the corresponding trends. Grey arrows indicate the number of days per year where the T - T_{NAT} < -1 K criterion was satisfied and DDU lidar was not operated.

G4) Section 4.1:
- The difference in ICE PSC occurrence needs more discussion. Tesche et al. (2021) shows an ICE occurrence of around 15% compered to 3.7% shown with P18. Could you please provide a pie chart from DDU for the same time period used in Tesche et al. (2021).
- Also, it would be good if you could provide a plot showing PSC occurrence per year (e.g. histogram). I would assume the ICE occurrence varies from year to year and that it was higher in the years 2015 and 2020, when the ozone hole set record sizes (see Stone et al. 2021).

The correlation between the 2015 and 2020 ozone hole is to our knowledge not proven to be specifically linked to ICE occurrences, even if they can both be the outcome of particularly cold polar winter seasons. It happens that 2015 and 2020 correspond to high aerosol burdens in the polar winter stratosphere following the Calbuco eruption and the Australian Black Summer that would probably be important parameter. As it was discussed in Tencé et al. (2022) the speciation between aerosol and PSC layers during such winters has to be cautious and would definitely make a distribution of PSC types for those winters significantly error prone. A recent publication from Ansmann et al., (2022) states on the increase of stratospheric ozone depletion from the influence of the carbonaceous aersols related to the australian wildfires by enhancing PSC formation. In addition, Rieger et al. (2021) investigated the correlation between the 2015 and 2020 strong ozone depletion years and presence of stratospheric global aerosol perturbation, either from a volcanic or a biomass burning event origin.

Though, the assumption on higher occurences of ICE clouds in both 2015 and 2020 at DDU is correct. However, ICE observations at DDU remain marginal due to the location of the station and as stated beforehand, we consider the yearly type distribution statistics would rely on too small samples to be reliable. The scope of our paper is the PSC detection at DDU from 2007 to 2020 and does not focus on specific years under aerosol perturbation influences. Still, specifically on the 2020 Australian event, Tencé et al. (2022), present the 2020 lidar observations at DDU, along with discussion on PSC occurrences as well as the ozone anomalies detected in October 2020 at DDU.

G5) Section 4.4. Why do you decide to use NCEP here? In the section before you concluded that NCEP has a T bias from 2k and ER5 should be used. ER5 and IASI should be used here.

NCEP is considered less accurate at DDU than ERA5. It still does not make the comparison proposed in Figure 9 useless. We are not using NCEP instead of ERA5, we are using both. And we modified Figure 9 to also include IASI as this was suggested by the reviewer. The inclusion of NCEP here adds valuable information in that, despite the discrepancies between datasets highlighted by figure 8, the 2 model and the spaceborne observationally derived trends are globally consistent. We choose therefore to keep it.

Minor comments:

1) Line 279: What threshold is used for background aerosol?

The background aerosol threshold used is R// = 1.06 as used in the original Blum et al. (2005) classification. It was indeed not specified in our manuscript, it was edited to explicitly mention this threshold: "The threshold separating PSC layers from background aerosols in B05 is R//,thresh = 1.06." lines **235-236**

2) Line 280: Sentence starting with: This might..... . Not clear what is being referred to.

"This might" was referring to choice of the threshold delimiting NAT clouds in B05. Another reviewer requested the rephrasing of this passage, we hope it is clearer now.

It was edited as follows, lines **360-363**: "Given the 10% depolarization threshold and the relatively low amount of NAT clouds identified by B05, we can consider that B05 classifies as NAT the PSCs that are only composed of, or highly dominated by NAT particles. Whereas P11 and P18 classes MIX1, MIX2 and NATmix correspond to NAT mixtures which may include a significant share of STS droplets."

3) Line 277: If you have a 3% crosstalk at DDU, would that not shift all the observation in Figure 3a slightly to the upper right corner?

Mentioning the crosstalk is part of the explanation about absence of measurement near the $R_\perp$ baseline. The estimation of 3% has been inherited from calibration at DDU in 2012 and we considered that it was small enough to be neglected in our data processing. Correcting crosstalk noise in lidar data processing is complex and is on the roadmap of future upgrades. To avoid confusion, this estimation is removed from the manuscript as it is not taken into account.

Edited line **358**: "For B05, the absence of measurements along the bottom x-axis is most likely the sign a small crosstalk noise."

4) Line 282: prominent share of NAT class among global Please add citation.

According to B05, 4.6% of the PSC detected at DDU are NAT clouds. We consider it is safe to say that this NAT share is very low as compared to other observations available in the litterature. Of course, most of the publications use PSC classification that do not include a pure NAT class, and rather use NAT mixtures classes such as P11 and P18. However, B05 was used in Blum et al. (2005) who found 15% of pure NAT and in Achtert et al. (2014) who found 13%. These numbers are roughly three times the NAT amount found at DDU. When using NATmixtures classes, Snels et al. (2019, 2021) and Pitts et al. (2018) find significant NATmixtures shares, at least above 30%. Following another reviewers' comment, we rephrased this sentence to make our point clearer. It does not include a statement on the share of NAT PSC among global observations anymore.

Edited, line **360-363**: "Given the 10% depolarization threshold and the relatively low amount of NAT clouds identified by B05, we can consider that B05 classifies as NAT the PSCs that are only composed of, or highly dominated by NAT particles. Whereas P11 and P18 classes MIX1, MIX2 and NATmix correspond to NAT mixtures which may include a significant share of STS droplets."

5) Line 285: not sure what is meant by that statement

Sentence actually needs to be rephrased ; we do not imply some direct correlation between latitude and optical properties, but rather that some range of optical properties need thermodynamical conditions rarely met at lower antarctic latitudes : ICE PSC persistence is related to temperature remaining below T_{ICE}, and our point is simply to state that optically equilibrated persistent ICE PSC layers are rarer above DDU than above stations at higher latitudes.

Edited in the manuscript to be clearer, lines **365-367**:
"The relative low number of ICE events we report relates to the fact ICE PSC fields above DDU are more unstable that those remaining deep inside the vortex. The optical properties of the ICE clouds observed at DDU are thus expected to be closer …."

6) Line 284: not clear. B05 has a small occurrence of pure NAT clouds, but NAT is included in MIX. And MIX is quite high in B05.
The MIX share in B05 is indeed significant. However, it is not designed as a NAT mixtures class. To quote B05, its definition of MIX is the following: "Here we will concentrate on the three classical types of PSC, Ia, Ib, and II, as well as on an additional type which comprises all data which do not fit one of the three classical types. We call this additional type of PSC 'mixed clouds'". Therefore, the MIX category includes NAT mixtures, but is not defined to explicitly gather these clouds and is not restricted to them.
Of course, when comparing the three classifications, we summed NAT+MIX for B05 in order to make the comparison possible with P11 and P18.

7) Figure 3. Add measurement date in the figure caption. Also, pleas add ɗ aer to B05.
The values shown in this figure correspond to all the PSC measurements detected at DDU between 2007 and 2020, it is now explicitly mentioned in the caption: **"… between 2007 and 2020".**
Concerning the δ_{aer} in this figure, it is explicitly featured in figure 2 to recall that the depolarization depends on $R_{//}$ and $R_{\perp}$. However, it is not included in figure 4 not to hinder visualization. We are not sure we understand the reviewers' request.

8) Line 305. Misleading. MIX is mixture if different types (STS, ICE and/or NAT), not a completely different typ of PSC
As pointed out in a response to a previous comment of the reviewer, here we just reminded how the MIX category is defined in B05, and we do not consider this category as a different type of PSC, so we are not sure to understand the reviewer's comment. Please note that B05, however, explicitly defines this MIX category as an additional type of clouds in the definition of the MIX category quoted above.
To make it clearer, we rephrased "… to any of the other types" into "… to any of the other classes" to explicit the fact that we are here referring to classification categories.
Edited line **395**: "classes"

9) Figure 4: Subplot a and b look the same, as well as d and e. Does that mean that STS and NAT+MIX between B05 and P11 agree very well? The bimodal distribution for ICE in B05 is very interesting. Could you provide the mean ɗ aer for the peaks?

The reviewer is right, STS and NAT+MIX between B05 and P11 agree very well. The figure was updated following the another reviewer's comment: the threshold temperatures are now calculated using the daily MLS H_2O and HNO_3 measurements. The present figure was sligthly modified due to this change. : the x-axis is now T - T_threshold, and not just the temperature. One can see that subplot a and b as well as d and e agree very well, with a slight difference for the NAT+MIX type.

About the bimodal pattern for ICE in B05, please note that on the updated figure it does not appear as clearly. This is due to the daily computation of T_{ICE}, that tends to decrease the threshold temperature value due to deshydratation during the winter. This consequently leads to disappearance of the "peak" of the distribution below T_{ICE} in the first version of the figure.

The figure shows the distribution of PSC measurements as a function of temperature and altitude. We are not sure to understand why there should be a coherence in term of depolarization values depending on the localisation of a point, i.e. in one "peak" of the distribution or another. Of course, non-zero depolarization values are expected at lower temperatures but there is no specific spatial consistency in term of depolarization values expected in such a (T,z) plan. Still, we separated the points in two groups according to these peaks, and they show approximately the same average depolarization value, around 7%.

10) Line 345: Really just the drift, not also the different resolution?
We do consider that the gap between ERA5 and the radiosonde temperatures is caused by the drift. ERA5 resolution in the stratosphere is acceptable and should not be at stake here. The resolution may be a problem around the tropopause : a low resolution and interpolation can cause discrepancies between a model and the radiosonde. ERA5 temperature fields of figure 6b and 6c show that temperatures are higher in the area where the balloon is around 15 and 17 km as compared to DDU. The drift of the sonde is way more likely to be causing this gap.
Looking at the ERA5 temperature fields at both one pressure level above 70 hPa and below 100 hPa (i.e. around 19 km and 13.5 km respectively), at 11PM both ERA5 and the radiosonde temperatures are much closer than on figure 6b and 6c, supporting the hypothesis about the radiosonde drift causing the temperature discrepancies combined to the local temperature variability.

11) Figure 5a: Looks very smooth. Too much interpolation? And the signal just above the tropopause is not classified. Why?
There was indeed a mistake and the applied smoothing was too strong, we thank the reviewer for noting this point, figure was updated to match the manuscript, i.e. smoothing on a 30 minutes window.

As it was extensively discussed in addressing comments from another reviewer, we apply a cloud layer detection method on the backscatter ratio as well as on the depolarization, whereas other datasets (CALIOP or Snels et al. (2021) adopt another approach. They sort each vertical individual bin applying a coherence criterium in order to avoid false detections. We chose to rely on a peak detection algorithm because we consider it safer to avoid false detection. This method still has drawbacks and we have to set the adequate parameters in order to detect the relevant layers in the signal: in some cases as this one pointed out by the reviewer, it can lead to an approximation in finding the borders of the layer. In this case, the bottom limit of the ICE PSC was not taken into account despite optical values that would have it classified among PSC. The choice of the method (bin by bin versus peak detection) is a compromise and both have disadvantages.

CALIOP data processing as presented in (Pitts et al., 2018) considers a bin as PSC when at least 11 of the neighbouring bins in a 3D box defined as 3 vertical bins per 5 horizontal bins around the candidate also share the same status. It also considers the status of this same bin with different horizontal averaging. There is no direct translation of this methodology to a groundbased dataset as it lacks the horizontal dimension. We consider that applying a coherence criterium only on the vertical dimension of one profile would be more prone to false detection and this is why we prefer the peak detection algorithm.

We consider safer not classifying a small amount of PSC bins and still ensuring statistical accuracy in pinpointing the type of main layer, than integrating false detections due to an imperfect coherence criterium, missing the horizontal awareness.

We also precise that the Figure 6b was modified to account for the change made in the PSC counting method when integrating CALIOP measurements in Figure 3. This change was described in our response to the comment G3 above. As one can see, it slightly changes the types identified on the left end of Figure 6b.

Here is the new version of Figure 6:

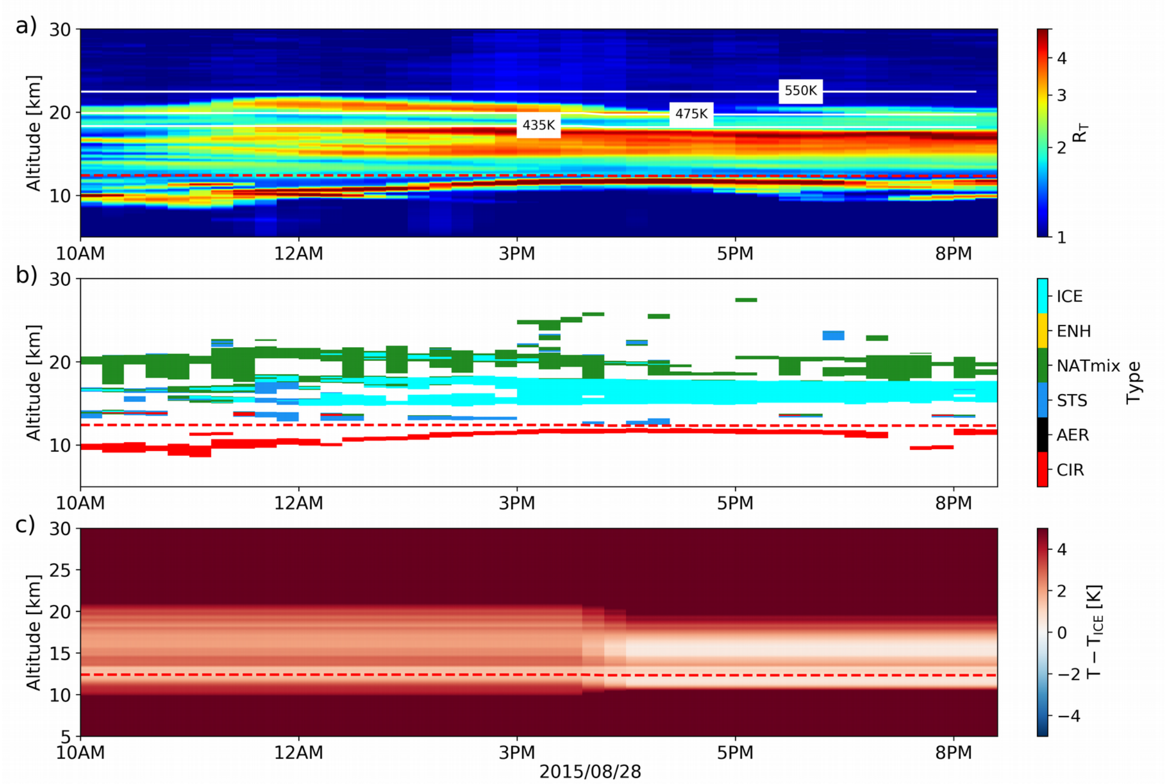

Figure 6: 32 nm backscatter ratio of lidar measurements obtained at DDU on the 2015/08/28 (a). The corresponding PSC types according to P18 classification scheme (b) and ERA5 temperatures at DDU as compared to the ICE formation threshold T_{ICE}, calculated from the MLS H_2O of the day (c). The red dashed line indicates the dynamic tropopause computed from ERA5 data.

12) Line 384: For the temperature comparison. What resolution were used? Did you interpolate the radiosonde profile on ER5, IASI, and NCEP?
For the temperature comparisons around line **469**, all temperature profiles were interpolated on a altitude grid shared between ERA5, IASI and NCEP, ranging from the surface up to 35 km with a 300 m resolution.

13) Section 4.4 and Figure 8. A discussion about the year to year variability of the ozone hole and PSC occurrence should be added here. For example, you could add a second y-axis showing the average ozone hole area for every year.
Inclusion of the ozone hole area in the figure would involve analysis at a scale different from the one considered in the scope of the current paper, which is the close vicinity around the station. Ozone hole area actually involves characterization of the polar vortex over the years, and the shifts, splits (due to sudden stratospheric warming events) and other feature related to the persistence and shape of the vortex are to be investigated and clearly complex enough to be a paper on its own.

Finally, and as discussed in the other reviews, this figure embeds a substantial amount of information. We thus hope the reviewer understands us being reluctant to add a dimension encompassing a scale broader to the one covered by our groundbased measurements.

It is important to note that the stratospheric denitrification is now taken into account in the T_{NAT} computation, and it tends to decrease T_{NAT} values. As a result, the ΔT criteria adujsted to our lidar measurements is now -1 K and not -2 K as in the initial version of the manuscript. Figure 9 and the associated discussion have been edited on lines **490** and **492** and in the caption of Figure 9.

14) Figure 9: What would be the thickness for your definition ($T-T_{NAT} < -2$ K). Would the model thickness agree than better with the observation?
In building the trend, we adjust the threshold ΔT so that the number of days meeting the criterion for lidar operation days matches the number of PSC observations at DDU. We emphasize on not reading this as a corrected formation temperature for PSC. It is a criterion enabling the use of temperature reanalyses as a proxy. Nonetheless, the reanalysis temperature uncertainties are necessarily accounted for into this criterion.

For example, ERA5 is not entirely expected to resolve subscale temperature variations enabling PSC formation, like orographically induced waves, even if most of the time not relevant above DDU.

Please note that the figure is now also edited following another reviewer's comment. First, the T_{NAT} values used in this figure account for the daily MLS H_2O and HNO_3 measurements, like it is now the case throughout the manuscript. The distribution plotted in the updated version of figure 10 is the stratospheric range satisfying T-Tnat **not** filled with PSC layers, this change should make it clearer to read. In the initial version, we computed the stratospheric range satisfying $T-T_{NAT}$ for each PSC detection as well as the PSC geometrical thickness, both being plotted. In order to avoid misinterpretation, we now plot the difference between the latter two. We think that this change better highlights our point.

As answer to the reviewer's final suggestion, we compute the same plot with T-Tnat←2K (now -1 K), and attach it below. As expected, the stratospheric range satisfying T-Tnat<-2K (now -1 K) not occupied by PSC layers appears smaller than the one from the figure in the paper but remains around 3-4 km on average. To address the reviewer’s comment as well as well taking the new ΔT into account, we provide below the figures for ΔT=0 K; -1 K and -2 K.

ΔT = 0 K

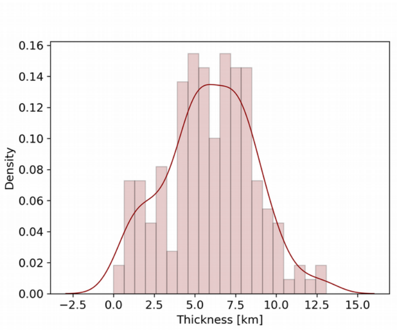

ΔT = -1 K

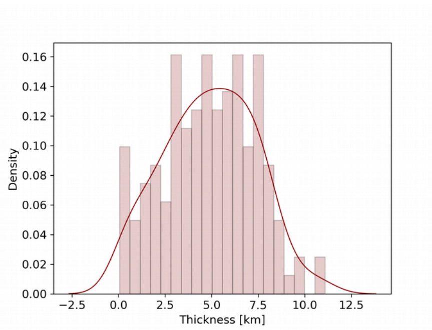

ΔT = -2 K

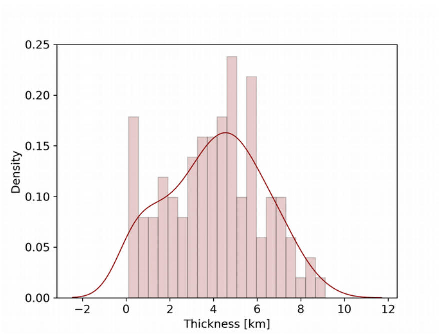

Figures are to small and of low quality
All figures are now made larger in the revised manuscript. Concerning the quality, all the figures were saved with the required dpi.

Suggested reference (Stone et al., 2021) along with Rieger et al. 2021, discussing the interplay between ozone depletion and stratospheric ozone has been added at line **31**.

References:

Ansmann, A., Ohneiser, K., Chudnovsky, A., Knopf, D. A., Eloranta, E. W., Villanueva, D., Seifert, P., Radenz, M., Barja, B., Zamorano, F., Jimenez, C., Engelmann, R., Baars, H., Griesche, H., Hofer, J., Althausen, D., and Wandinger, U.: Ozone depletion in the Arctic and Antarctic stratosphere induced by wildfire smoke, Atmospheric Chemistry and Physics, 22, 11 701–11 726, https://doi.org/10.5194/acp-22-11701-2022, 2022.

Rieger, L. A., Randel, W. J., Bourassa, A. E., and Solomon, S.: Stratospheric Temperature and Ozone Anomalies Associated With the 2020 Australian New Year Fires, Geophysical Research Letters, 48, e2021GL095 898, https://doi.org/https://doi.org/10.1029/2021GL095898, e2021GL095898 2021GL095898, 2021.

Snels, M., Scoccione, A., Di Liberto, L., Colao, F., Pitts, M., Poole, L., Deshler, T., Cairo, F., Cagnazzo, C., and Fierli, F.: Comparison of Antarctic polar stratospheric cloud observations by ground-based and space-borne lidar and relevance for chemistry–climate models, Atmospheric Chemistry and Physics, 19, 955–972, https://doi.org/10.5194/acp-19-955-2019, 2019.

Snels, M., Colao, F., Cairo, F., Shuli, I., Scoccione, A., De Muro, M., Pitts, M., Poole, L., and Di Liberto, L.: Quasi-coincident observations of polar stratospheric clouds by ground-based lidar and CALIOP at Concordia (Dome C, Antarctica) from 2014 to 2018, Atmospheric Chemistry and Physics, 21, 2165–2178, https://doi.org/10.5194/acp-21-2165-2021, 2021.

Stone, K. A., Solomon, S., Kinnison, D. E., and Mills, M. J.: On Recent Large Antarctic Ozone Holes and Ozone Recovery Metrics, Geophysical Research Letters, 48, e2021GL095 232, https://doi.org/https://doi.org/10.1029/2021GL095232, e2021GL095232 2021GL095232, 2021.